# IM7/LARC$^{TM}$-ITPI polyimide composites*

**T. H. Hou and E. J. Siochi**
*Lockheed Engineering & Sciences Company, Hampton, VA 23666, USA*

**and N. J. Johnston† and T. L. St. Clair**
*NASA Langley Research Center, Hampton, VA 23681-5225, USA*

LARC$^{TM}$-ITPI, an isomeric variation of the better known LARC$^{TM}$-TPI and based on 4,4'-isophthaloyldiphthalic anhydride and 1,3-phenylenediamine, was evaluated as a matrix for high-performance composites. Five 30% poly(amide acid) solutions in *N*-methyl pyrrolidone, with stoichiometric offsets of 2.0, 3.0, 4.0, 4.75 and 5.5% in favour of the diamine and end-capped with phthalic anhydride, were synthesized and their molecular weights and molecular weight distributions determined. Importantly, high concentrations of low molecular weight species were found in all the offset compositions. Solvent/volatile depletion rates were carefully determined on thermally imidized films of the five compositions and were an important part of the composite consolidation studies. All films failed a solvent resistance test which involved immersion in acetone, methyl ethyl ketone, toluene, dimethylacetamide and chloroform for 1 min followed by a fingernail crease. A minor modification of the polymer backbone improved solvent resistance measurably. Unidirectional IM7 prepreg was made from each of the five resin solutions by standard drum-winding procedures. A workable composite consolidation cycle was developed for the 3% offset solution by conducting a parametric study involving residual solvent content, melt viscosity and composite C-scan information. The basic strategy was to B-stage the prepreg to a temperature where 98% of the volatiles were depleted while, at the same time, adequate molten resin fluidity (via incomplete imidization and residual solvent content) was retained, then apply pressure and increase temperature to complete the consolidation. This moulding cycle was then applied successfully to the remaining compositions and composites fabricated. From the processing information and composite mechanical properties, including short-beam shear strength, flexural strength and flexural modulus at room temperature, 93, 150 and 177°C, the 4.75% stoichiometrically offset end-capped polymer was chosen as the optimal matrix. Composite engineering properties for this selected composition were also obtained, including longitudinal tension, transverse flexural, longitudinal compression, interlaminar shear, short-block compression, compression strength after impact and open-hole compression (OHC). Notably, 80% of the room temperature OHC strength was retained at 177°C, indicating that the LARC$^{TM}$-ITPI is an excellent high-temperature matrix material for selected future aerospace applications where solvent resistance is not a key requirement.

**(Keywords: polyimide; composite; mechanical properties)**

## INTRODUCTION

Aromatic polyimides have long been recognized as attractive for applications in the aerospace and electronic industries. The high glass transition temperatures, $T_g$, offered by these polymers are attributed to the stiff molecular backbones which contain aromatic rings. Such structures lead to unique properties such as thermal and thermo-oxidative stability at elevated temperatures, superior chemical resistance and excellent mechanical properties.

One of the major problem areas for this class of polymers is poor processability. In fully imidized forms, many are insoluble in most organic solvents and usually infusible at elevated processing temperatures. Consequently, in most applications a precursor poly(amide acid) solution in a high boiling polar solvent must first be prepared and then converted thermally to polyimide. During the thermal imidization reaction, some reaction volatiles are inevitably generated and extra care is required in the development of a consolidation moulding cycle (temperature and pressure profiles) to ensure a void-free end product. These characteristics have limited the applications of this class of polymers.

One of the well known high performance thermoplastic polyimides is LARC$^{TM}$-TPI developed by NASA Langley Research Center in the late 1970s and sold commercially under license by MTC, Inc.[1]. In order to improve the melt-flow properties for this material, various approaches have been investigated in the past. Extensive molecular structure modifications have been performed[2-8]. It was found that introduction of flexible linkages such as $-CH_2-$, $-O-$, $-SO_2-$ into the backbone, together with the use of *meta*-substituted diamines, often leads to enhanced thermoplasticity. Other approaches included the doping of low molecular weight diimide additives[9,10] and slurry blending of different polymers[11-13]. Perhaps the most successful approach was to control molecular weight by end-capping[14]. All these approaches have resulted in various degrees of success in enhancing the polymer melt

*Presented at the American Chemical Society, Division of Polymer Chemistry '17th Biennial Symposium on Advances in Polymerization and High Performance Polymeric Materials', 22–25 November 1992, Palm Springs, CA, USA

This work was performed at NASA Langley Research Center, Hampton, VA, USA. This paper is declared a work of US government and is not subject to copyright protection in the United States

†To whom correspondence should be addressed

0032-3861/94/23/4956–14

processability while retaining properties inherent to polyimides.

A $C_{30}H_{14}N_2O_6$ isomeric variation of LARC™-TPI was recently developed and designated as LARC™-ITPI[15-17]. It is based on 4,4'-isophthaloyldiphthalic anhydride (IDPA) and 1,3-phenylenediamine (*m*-PDA), a commercially available diamine. The structures of these two isomeric polyimides are shown in *Figure 1*.

In order to evaluate this new polymer as a composite matrix, five end-capped LARC™-ITPI resins with various theoretical (formulated) molecular weights (*TMW*) were scaled up and used to fabricate unidirectional carbon fibre prepreg. This paper expands our previous initial study and presents the design of a workable moulding cycle for consolidation of this prepreg[18]. A full set of engineering mechanical properties of the resultant composites and processing–composite property– molecular weight relationships will be given.

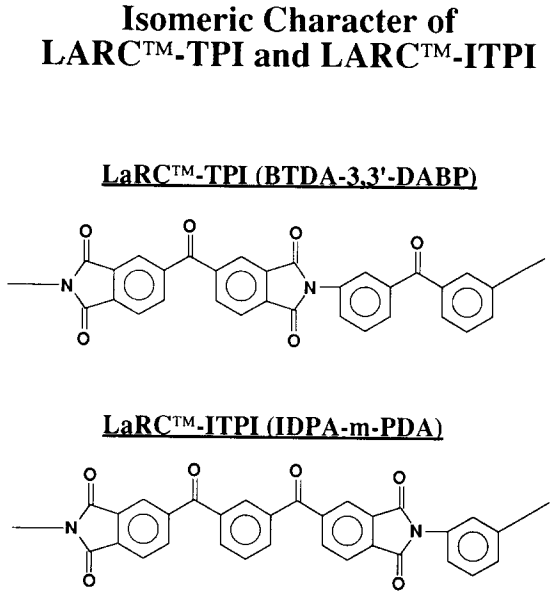


**Figure 1** Chemical structures of LARC™-TPI and LARC™-ITPI

## EXPERIMENTAL‡

The *m*-PDA was obtained from Du Pont, Wilmington, DE, and used as received. The IDPA was supplied by Imitec, Inc., Schenectady, NY, at 98.5% purity. Five poly(amide acid)s with stoichiometric offets of 2.0, 3.0, 4.0, 4.75 and 5.5% in favour of *m*-PDA were synthesized as tabulated in *Table 1*. All were end-capped with phthalic anhydride (PA). Monomers were reacted to form 30% w/w solutions in *N*-methylpyrrolidone (NMP); the reaction chemistry is shown in *Figure 2*. The polymer solutions were stored in a freezer at −4°C until use.

Molecular weight distributions of the poly(amide acid) solutions were obtained using a Waters 150C gel permeation chromatograph equipped with a differential refractive index detector connected in parallel configuration with a Viscotek model 150R differential viscometer (g.p.c./d.v.). Experiments were conducted in distilled

‡Use of trade names or manufacturers does not constitute an official endorsement, either expressed or implied, by the National Aeronautics and Space Administration

**Table 1** Formulation of LARC™-ITPI polymers

| Stoichiometric offset (%) | Molar ratio IPDA[a]:*m*-PDA:PA | *TMW*[b] (g mol$^{-1}$) |
|---|---|---|
| 2 | 0.995:1.0:0.040 | 25146 |
| 3 | 0.985:1.0:0.060 | 16688 |
| 4 | 0.975:1.0:0.080 | 12446 |
| 4.75 | 0.967:1.0:0.095 | 10440 |
| 5.5 | 0.959:1.0:0.110 | 8992 |

[a]98.5% purity
[b]Theoretical (formulated) molecular weight

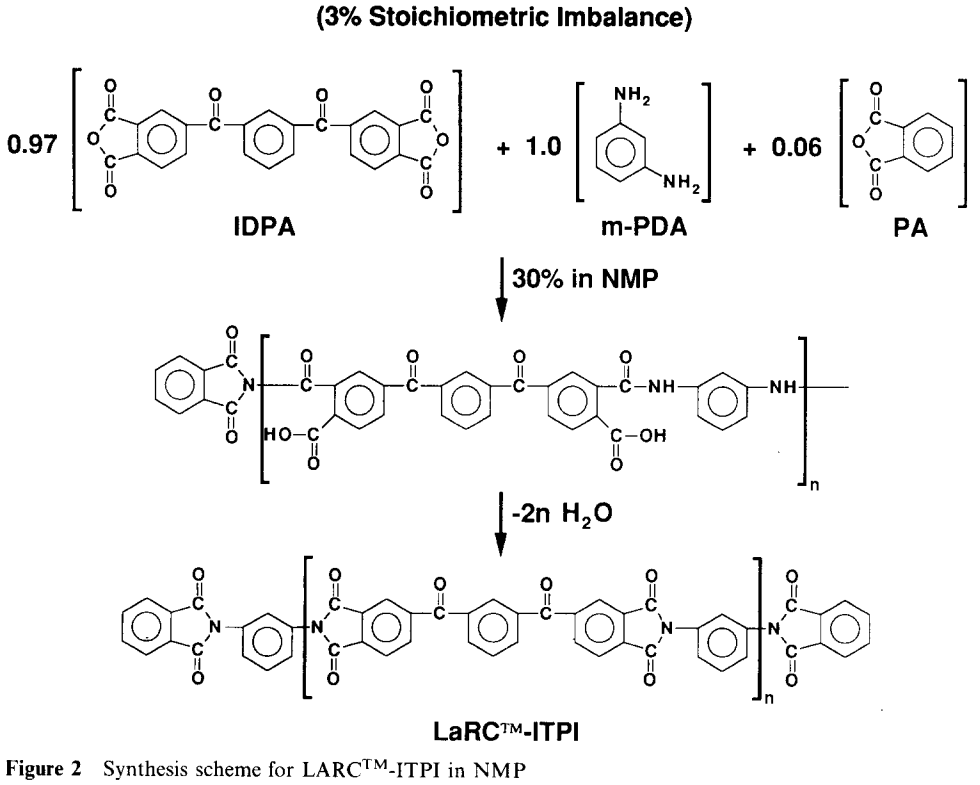


**Figure 2** Synthesis scheme for LARC™-ITPI in NMP

NMP containing 0.02 M $P_2O_5$ at 60°C on a Permagel column bank consisting of 500, $10^3$, $10^4$, $10^5$ and $10^6$ Å columns at a flow rate of 0.9 ml $min^{-1}$. Care had to be taken to distil the NMP, filter the solvent after it was stirred over $P_2O_5$ for about 30 min and degas the solvent before sample preparation and chromatography. The dilute solutions were prepared, held at 60°C for 45 min, filtered through a 0.2 $\mu$m Teflon filter and injected. Duplicate runs were done using freshly prepared solutions.

Polyimide films were prepared as follows. A 30% w/w poly(amide acid) solution of LARC$^{TM}$-ITPI in NMP was doctored onto a glass plate and the film cured for 1 h at each temperature of 100, 200 and 300°C in a forced-air circulating oven. Portions of each film were further post-cured for 1 h each at either 350, 371 or 400°C. Thicknesses varied from 76.2 to 127 $\mu$m. Glass transition temperatures ($T_g$) of the films were determined on a Du Pont 1090 Thermal Analyzer using a heating rate of 20°C $min^{-1}$. Weight loss was determined on a Seiko TG/DTA model TGA747 instrument in air at a temperature ramp of 2.5°C $min^{-1}$ from 100 to 650°C.

Solvent resistance experiments were conducted as follows. Fully imidized film was cut into strips of approximately 5.08 cm in length and 0.635 cm in width, bent along the length and the round tip immersed in solvent for 1 min at room temperature (r.t.). The effect on the film was examined either by observation or by fingernail creasing. Five solvents were employed: acetone, methyl ethyl ketone (MEK), toluene, *N*,*N*-dimethyl-acetamide (DMAc) and chloroform.

Rheological properties of the neat polymers were determined using a Rheometrics System 4 rheometer fitted with a parallel plate fixture. Films were moulded at 300°C into 2.54 cm diameter discs 1.10–1.30 mm thick. Isothermal runs were performed with the test chamber prewarmed to the measurement temperature. During the run, the top plate was oscillating at 10 rad $s^{-1}$ while the bottom plate (mounted on a torque transducer) remained stationary. A strain of 1–5% was selected in order to generate adequate torque levels and, at the same time, maintain a linear viscoelastic response. Torque was decomposed into in-phase and out-of-phase components which correspond to the elastic ($G'$) and loss ($G''$) moduli, respectively, for the measured specimen.

Unidirectional prepreg was produced from Hercules IM7 12K unsized graphite fibre by standard drum winding procedures using the 30% poly(amide acid) solutions in NMP. The wet prepreg was heated on the drum overnight at 90°C, followed by an oven B-stage at 250°C for 1.0 h and stored at r.t. until use. The dried plies were trimmed to size and stacked in a closed steel mould between Kapton film spray-coated with Frekote 33. Two layers of bleeder cloth were employed on each side of the laminate. Moulding was done in a 22 650 kg four-post upacting press containing 30.5 $cm^2$ electrically heated platens. Heating and cooling rates of about 7°C $min^{-1}$ were employed. Panels were evaluated ultrasonically at a pre-established sensitivity level adequate to detect microvoids in carbon fibre/epoxy composites. Resin weight fraction for each specimen was determined by acid digestion in a 1:1 w/w concentrated sulfuric acid: 30% hydrogen peroxide mixture.

Composite mechanical properties were measured at r.t. and elevated temperatures in accordance with standard ASTM procedures. Tension tests were performed at a constant stroke of 0.127 cm $min^{-1}$ in a 22.3 kN electro-hydraulic test machine equipped with hydraulic grips. All compression tests were performed in a 53.5 kN hydraulic test machine at a constant rate of 0.127 cm $min^{-1}$. Specimens were instrumented with 350 Ω back-to-back strain gauges. Data were gathered with a 16-bit resolution A/D microcomputer-based data acquisition system. Standard IITRI procedures were employed for the unidirectional compression tests while short-block compression (SBC) tests utilized a specimen configuration and fixture developed at NASA Langley to prevent brooming-type failures.

Open-hole compression (OHC) properties and compression strength after impact (CAI) were performed according to Boeing Document D6-55587 and BSS 7260. The CAI specimen was clamped between steel plates containing 7.62 cm × 12.7 cm centre cutouts. A 1.58 cm diameter spherical-tip indenter was dropped to yield a normalized impact energy of 682 cm kg of energy per cm of specimen thickness. The impacted specimens were C-scanned before compression testing to determine the nature and extent of the impact damage. The compression test fixture utilized clamped ends to prevent brooming failures and simple support knife edges on each side.

OHC measurements at r.t. and 177°C were conducted at the University of Wyoming, Laramie, WY. The specimen was 30.5 cm long, 3.8 cm wide with a 0.635 cm diameter hole in the centre. A Measurements Group EA-06-125BB-120 single-element strain gauge was bonded to the specimen 2.54 cm below the hole. Tests were performed at a crosshead speed of 0.127 cm $min^{-1}$ in a Boeing-designed fixture using an Instron model 1334 test machine. A Bemco FTU 3.0 environmental chamber was used for the 177°C tests. Each specimen was conditioned in the chamber for approximately 30 min prior to testing.

Interlaminar fracture toughness, $G_{IC}$, was measured by double cantilever beam (DCB) method at r.t. Test specimens were nominally 2.54 cm wide, 15.2 cm long, and between 0.318 and 0.368 cm thick. A 2.54 cm long Kapton insert at the specimen mid-plane at one end of the specimen (placed during laminate fabrication) facilitated crack initiation and extension. Piano hinges were bonded to the ends of specimens for load introduction. The bonds were reinforced with small strips of steel shim stock wrapped around the specimen and hinge. An Instron 1125 universal testing machine with conventional mechanical wedge-action grips and a universal joint in the load train was employed. A crosshead speed of 2 mm $min^{-1}$ was used for the majority of tests, although crosshead speed had no discernible effect upon the results. The area under the load–displacement curve was measured manually. The area method[19] was used to calculate the critical strain energy release rate, $G_{IC}$, for each crack extension.

## PHYSICAL PROPERTIES OF LARC$^{TM}$-ITPI SOLUTIONS AND NEAT POLYMERS

### *Poly(amide acid) solution properties*

Solution properties of the 30% poly(amide acid) solutions in NMP are tabulated in *Table 2* and the molecular weight distributions given in *Figure 3*. Except for the 5.5% offset polymer, the number average molecular weights, $M_n$, decreased as a function of the increase in stoichiometric offset, as expected. However, the measured values were lower than the theoretically calculated number average molecular weight (i.e. *TMW*,

**Table 2** Solution properties of LARC™-ITPI in NMP

| Stoichiometric offset (%) | $M_n$[a] (g mol$^{-1}$) | $M_w$[a] (g mol$^{-1}$) | $M_w/M_n$ | Inherent viscosity[b] (dl g$^{-1}$) $\eta_{inh}$[c] | $\eta_{inh}$[d] | $\eta_{inh}$[e] | $[\eta]$[f] (dl g$^{-1}$) | $\eta$[g] (Pa s (cP)) |
|---|---|---|---|---|---|---|---|---|
| 2 | 15465 | 35190 | 2.28 | 0.44 | 0.513 | 0.426 | 0.323 | 21.5 (21500) |
| 3 | 11600 | 31415 | 2.71 | 0.43 | 0.442 | 0.365 | 0.313 | 13.0 (13000) |
| 4 | 10975 | 24945 | 2.27 | 0.39 | 0.374 | 0.331 | 0.274 | 7.5 (7500) |
| 4.75 | 10135 | 23700 | 2.34 | 0.35 | 0.346 | 0.307 | 0.264 | 5.4 (5400) |
| 5.5 | 10967 | 23383 | 2.13 | 0.29 | 0.330 | 0.300 | 0.244 | 4.6 (4600) |

[a]Averaged molecular weights measured from dilute solution in NMP 0.02 M $P_2O_5$ by g.p.c./d.v. at 60°C
[b]Inherent viscosity measured in 0.5% dilute NMP solution at 35°C
[c]Provided by manufacturer (Imitec, Inc)
[d]Measured on 30% solutions in NMP as received
[e]Measured on residual 30% NMP solution after prepregging
[f]Intrinsic viscosity at 60°C by g.p.c./d.v.
[g]Brookfield viscosity of 30% w/w solutions at r.t.

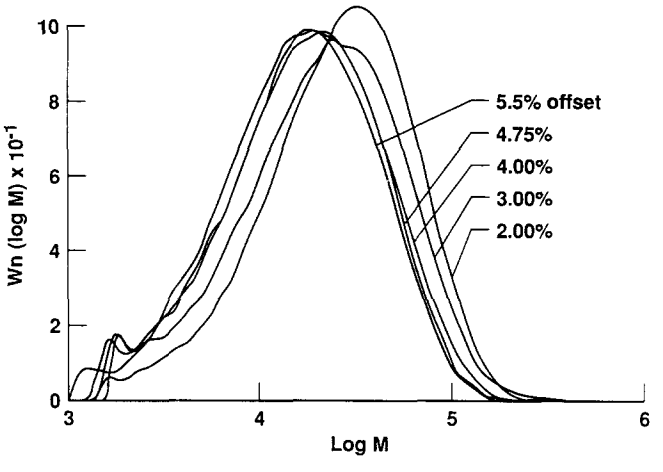


**Figure 3** Dilute solution viscosity *versus* theoretical molecular weight for the five LARC™-ITPI poly(amide acid)s in NMP

*Table 1*). This discrepancy may be attributed to the presence of some low molecular weight (*LMW*) species in all polymers as the data in *Figure 3* indicate. The data also suggest that higher concentrations of *LMW* species are present in polymers with lower stoichiometric offsets, resulting in a greater deviation from the theoretical values. Probably for the same reason, a similar trend was observed for the polydispersities, $M_w/M_n$, tabulated in *Table 2*; the measured polydispersity values converged toward the theoretical value of 2.0 as the stoichiometric imbalance increased. The implications for composite processing are obvious. At offset stoichiometries of 4–4.75%, the molten polymers process very well, probably because of the relatively high concentration of *LMW* species. For these compositions, the $M_n$ values are still reasonably high for achieving good mechanical properties.

Inherent viscosity decreased, as expected, with decreasing *TMW* (*Table 2*). For the fresh poly(amide acid)s, except for the 2% offset material, the inherent viscosities provided by the manufacturer were similar to those measured on the 30% solutions as received in our laboratory. For the residual 30% poly(amide acid) solutions collected after being exposed to ambient temperature for 4 h during prepregging operations, the inherent viscosities were consistently lower than those for the fresh polymers. A similar but much more severe trend was also observed for the dilute solutions of these poly(amide acid)s; a 50% drop in the intrinsic viscosity was observed over a 10 h span[20]. Such a pronounced rate of decrease in molecular weight might be caused by the chemical structure of poly(amide acid)s and will be the subject of future work. Similar behaviour on dilute solutions of other poly(amide acid)s has been observed[21,22]. The fact that the viscosity of the 30% solutions dropped as a result of exposure during the prepregging operation indicates that the polymer is undergoing significant changes under ambient conditions at 30% in NMP and that one should be careful about the length of time the polymer solution stands at r.t. while awaiting and after prepregging. This observation contrasts with that observed by Kilhenny and Cercena[23] who found no molecular weight decrease in 7.5, 15 and 30% solutions of LARC™-TPI poly(amide acid)s in NMP at 21°C under carefully controlled conditions. However, in the prepregging operation employed in this study, no attempt was made to exclude the absorption of atmospheric water whose presence may cause hydrolysis and concomitant decrease in viscosity. A second explanation may be that the poly(amide acid)s are equilibrating to a lower viscosity under ambient prepregging conditions. Such re-equilibration has been addressed by Volksen and Cotts on concentrated poly(amide acid) in NMP[24].

As part of the dilute solution characterization of the five poly(amide acid)s, the Mark—Houwink–Sakurada constants were determined using the following equation:

$$\log [\eta] = \log k + a(\log M_w) \quad (1)$$

The intrinsic viscosities were those obtained with the g.p.c./d.v. The molecular weight was the weight average molecular weight since this parameter is typically 1.1–1.25 times the value of the viscosity average molecular weight, the quantity that actually appears in the Mark–Houwink–Sakurada equation. The Mark–Houwink plot is shown in *Figure 4*. The data for the five polymers fell on a reasonably linear straight line with a correlation coefficient of 0.96. For randomly coiled polymers with linear-flexible backbones, the exponent $a$ lies between 0.6 and 0.8 and typical values of $k$ range between 0.5 and $5 \times 10^{-4}$ (ref. 25). The $a$ and $k$ constants obtained for the poly(amide acid)s suggest that at 60°C in distilled NMP/0.02 M $P_2O_5$, these molecules behave like randomly coiled polymers with linear flexible backbones.

Relationships between stoichiometric offset and both *TMW* and Brookfield viscosity for the five polymers are shown in *Figure 5*. Both the viscosity and *TMW* increase

dramatically as the stoichiometric offset decreases below 4%. This was probably the reason why the 2% offset solutions were more difficult to prepreg. Fibre bundles were not fully wetted and impregnated.

*Solvent resistance*

Poly(amide acid) films were cast and given a variety of thermal histories for several characterization studies. First, resistance to five solvents — acetone, MEK, toluene, DMAc and chloroform — was determined. These data on cured and post-cured films with stoichiometric imbalances of 3 and 4.75%, along with $T_g$ values, are tabulated in *Table 3*. After immersion for 1 min in solvent, the films remained intact. However, most were not fingernail creasable, even after various post-cure treatments at either 350, 371 or 400°C. However, as expected, $T_g$ values increased about an average of 10°C as a result of the thermal exposure, and the lower the offset stoichiometry (higher molecular weight) the higher the $T_g$.

To try to improve solvent resistance in the LARC™-ITPI polymer, the effect of backbone alteration was studied by replacing the *m*-PDA with *p*-PDA at 10 and 20% levels in the 3% offset polymer. Generally, resistance to acetone, MEK and toluene improved (*Table 3*). The results in DMAc and chloroform were the same as for the unmodified composition. This seemingly minor change in backbone structure has been successfully applied to other polyimides, affording significant improvements in solvent resistance[26].

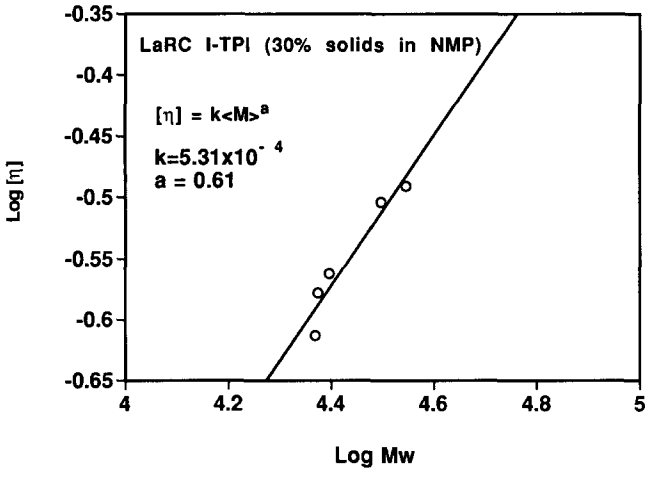


**Figure 4** Mark–Houwink plot for LARC™-ITPI poly(amide acid)s in NMP

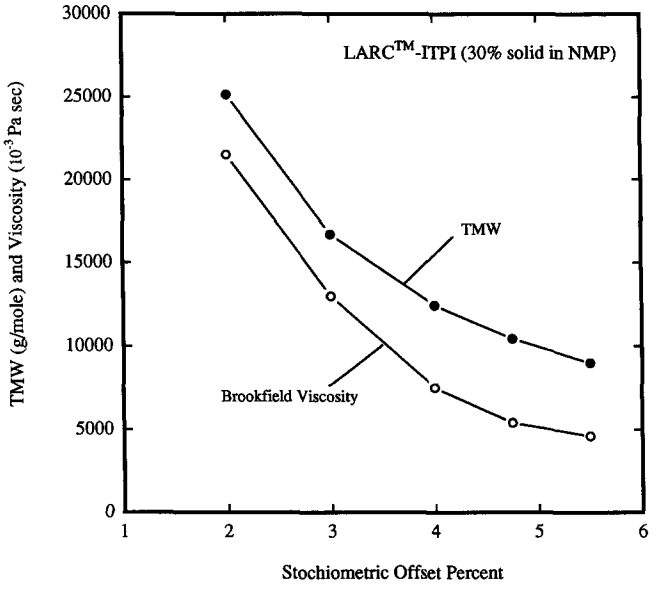


**Figure 5** Theoretical molecular weight and Brookfield viscosity *versus* stoichiometric offset for LARC™-ITPI poly(amide acid)s in NMP

**Table 3** Solvent effect on LARC™-ITPI polymer films[a]

| Cure temp. (°C)[b] | Resin system | $T_g$ (°C) | Control[c] | Acetone | MEK | Toluene | DMAc | Chloroform |
|---|---|---|---|---|---|---|---|---|
| 300 | 4.75% offset | 243.6 | +[d] | + | + | + | + | + |
| | 3% offset | 246.5 | −[e] | + | + | + | + | + |
| | 3% offset, 10% *p*-PDA | 252.9 | − | − | + | + | + | + |
| | 3% offset, 20% *p*-PDA | 253.7 | − | − | + | + | + | + |
| 350 | 4.75% offset | 256.4 | + | + | + | + | + | + |
| | 3% offset | 260.8 | + | + | + | + | + | + |
| | 3% offset, 10% *p*-PDA | 264.6 | − | − | + | − | + | + |
| | 3% offset, 20% *p*-PDA | 259.9 | − | − | − | − | + | + |
| 371 | 4.75% offset | 254.0 | + | + | + | + | + | + |
| | 3% offset | 260.3 | + | + | + | + | + | + |
| | 3% offset, 10% *p*-PDA | 266.2 | − | − | − | − | + | + |
| | 3% offset, 20% *p*-PDA | 264.5 | − | − | − | − | + | − |
| 400 | 4.75% offset | 259.5 | + | + | + | + | + | + |
| | 3% offset | 263.0 | + | + | + | + | + | + |
| | 3% offset, 10% *p*-PDA | 279.9 | + | + | + | + | + | + |
| | 3% offset, 20% *p*-PDA | 278.8 | + | + | + | + | + | + |

[a]Film was cast from 30% solid poly(amide acid) solution in NMP. Experiment was conducted by immersing the imidized film in solvent for 1 min. The film with width 12.7 mm and thickness 0.076–0.127 mm was bent along its length during the experiment

[b]Film was cured at the indicated final curing temperature for 1 h. Complete thermal history included additional curing of 1 h each at 100, 200 and 300°C in all cases

[c]As-cured film (no contact with solvent) behaviour

[d]+, Fingernail creasable at r.t. before or after immersion

[e]−, Shattered by fingernail creasing at r.t. before or after immersion

*Solvent removal studies*

Conditions required to remove NMP during the moulding operation were determined by d.s.c. and t.g.a. studies on thermally treated films of the 3% offset polymer solution. Films initially dried at 150°C were further dried at 225, 250 and 300°C and weight loss measurements taken after each drying stage. The results are tabulated in *Table 4* and plotted in *Figure 6*. Complete solvent removal was only attained after thermal treatment at 300°C for 1 h (specimen D), as expected, yielding a $T_g$ of 255°C. Thermal treatments below 300°C were unable to remove the bulk of the solvent from the polymer and $T_g$ values of these films were significantly lower.

Temperatures at which 2 and 5% weight loss occurred were determined from the t.g.a. plots in *Figure 6* and tabulated in *Table 4*. For specimens A, B and C, the weight loss profile exhibited a two-step process: weight loss at lower temperatures was attributed to the loss of NMP; weight loss at the higher temperatures was attributed to the degradation of short-chain oligomers and/or polymers. A relatively flat plateau was observed between the two steps. For specimen A, both 2 and 5% weight loss occurred in the first step (at 176 and 201°C), a clear indication of predominant solvent loss instead of polymer degradation. As the thermal pretreatment temperature increased, the temperature at which 5% weight loss occurred increased towards the end of the flat plateau and into the second step, an indication of an increasing degree of material degradation as opposed to the loss of solvent. These results clearly delineated the temperature range to be employed in removing solvent and reaction volatiles from prepregs during B-stage and consolidation operations. They also indicated conditions which would leave desirable quantities of solvent in the prepreg, if needed, for purposes of plasticization of the polymer melt to aid polymer flow and consolidation.

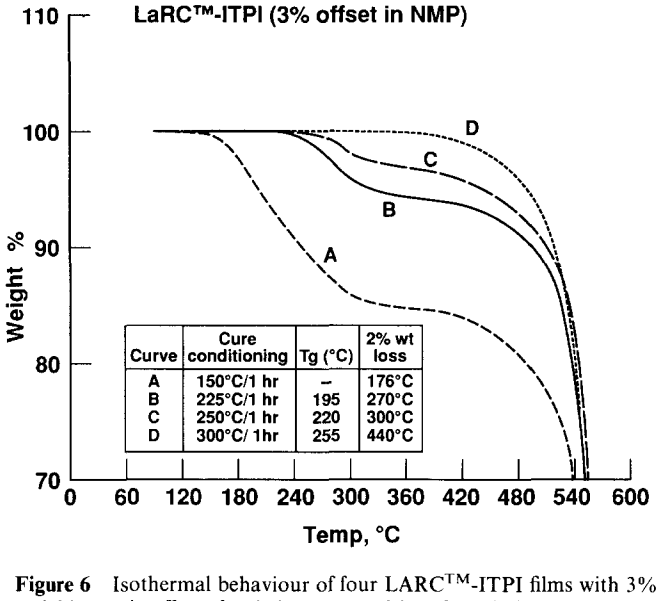


**Figure 6** Isothermal behaviour of four LARC™-ITPI films with 3% stoichiometric offset after being B-staged in a forced-air oven

**Table 4** T.g.a. results for the 3% offset films of LARC™-ITPI in NMP

| Specimen | Thermal treatment C | Thermal treatment h | $T_g$ (°C) | Temperature (°C) at 2% wt loss | Temperature (°C) at 5% wt loss |
|---|---|---|---|---|---|
| A | 150 | 1.0 | – | 176 | 201 |
| B | 225 | 1.0 | 195 | 270 | 340 |
| C | 250 | 1.0 | 220 | 300 | 440 |
| D | 300 | 1.0 | 255 | 440 | 485 |

*Rheological properties*

Rheological measurements were performed isothermally at 350°C under a fixed strain, $\varepsilon = 2\%$, and a fixed angular frequency, $\omega = 10\,\text{rad}\,\text{s}^{-1}$. Data for the five polymers are plotted in *Figure 7* as loss tangent (tan $\delta$) *versus* time ($t$). According to equation (2)

$$\tan\delta(\omega,t,T) = \frac{G''(\omega,t,T)}{G'(\omega,t,T)} \qquad (2)$$

tan $\delta$ is the ratio of the loss (dissipation, $G''$) and the storage (elastic, $G'$) moduli for a test specimen deformed under frequency $\omega$ at time $t$ and temperature $T$. When $\tan\delta > 1$ the specimen exhibits viscoelastic liquid-like behaviour; when $\tan\delta < 1$ the specimen exhibits viscoelastic solid-like behaviour. We have observed that polyimides and poly(arylene ether) matrices with tan $\delta$ values $> 1$ were relatively easy to thermoplastically mould into well-consolidated composites[27-30].

Values of $\tan\delta < 1$ were obtained at 350°C for all five fully imidized polymers. Despite the PA end-capping employed for molecular weight and melt viscosity control, the expected enhanced molten resin fluidity did not materialize. In addition, tan $\delta$ did not vary systematically with changes in *TMW*, apparently because of insufficient adhesion between the molten resin specimen and the fixture plates. This may have been due to the high stiffness of these fully imidized polymers at the measuring temperature. Although the values of $G'$ and $G''$ are inaccurate due to poor adhesion during the measurement, the conclusion that these materials possess viscoelastic solid-like behaviour can still be confidently made. It was also observed that these polymers were quite stable at 350°C during the measuring period.

Again, the implication for composite processing was obvious. The polymer probably could not be compression-moulded at reasonable temperatures and pressures while tan $\delta$ was $< 1$. Sufficient solvent would have to be retained during the consolidation phase to yield a polymer with $\tan\delta > 1$, thereby improving its melt processability significantly.

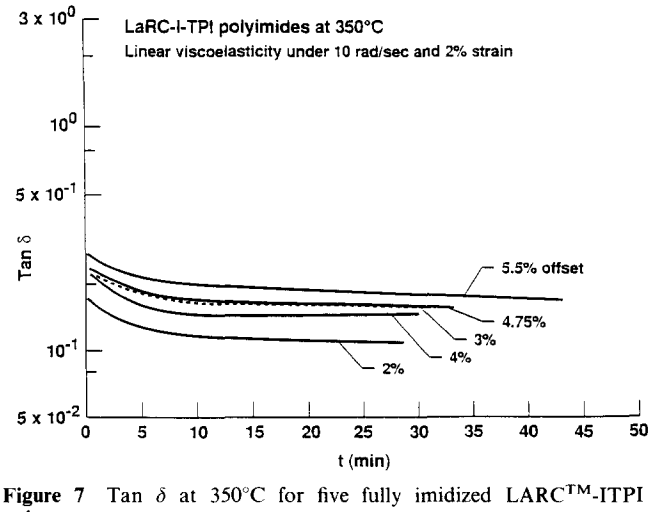


**Figure 7** Tan $\delta$ at 350°C for five fully imidized LARC™-ITPI polymers

## DESIGN OF A COMPOSITE MOULDING CYCLE FOR LARC™-ITPI PREPREG

Because of the difficulty in autoclave consolidation at high temperatures and pressures, the moulding cycle was restricted as follows: pressure, 1.72 MPa or less; temperature, 400°C or less. The design of a workable cure cycle for IM7/LARC™-ITPI under these guidelines represented a difficult challenge for the following reasons.

(1) When fully imidized, the matrix resin exhibited viscoelastic solid-like behaviour. It was unlikely that a pressure of 1.72 MPa would be able to force the molten matrix resin to infiltrate and fully consolidate the fibrous structure. Consequently, the full consolidation pressure would have to be applied before the matrix resin reached its fully imidized state in order to take advantage of (a) the higher degree of melt fluidity in the residual poly(amide acid) and (b) the presence of solvent which would plasticize the matrix thereby increasing melt flow.
(2) The processing window was therefore restricted to a narrow range in temperature and time in which a balance would be reached between the depletion of volatiles (solvent and reaction by-products) and the loss of melt fluidity of the reactive matrix resin. For the LARC™-ITPI/NMP resin system, the similarity between the boiling point of the solvent (200°C) and the imidization temperature range for the poly(amide acid) made the processing window even more difficult to define.

Consequently the following guidelines were used for designing a moulding cycle for the IM7/LARC™-ITPI/NMP system.

(1) The amount of residual NMP in the prepreg before applying the consolidation pressure was arbitrarily targeted at 2% w/w. The amount remaining in the final consolidated part and its effect on composite properties is not known and can only be estimated.
(2) From the behaviour of specimen D (e.g. *Figure 6* and *Table 4*), it appears that polymer degradation occurred at temperatures above 440°C. Therefore, the thermal history of specimen D (300°C/1 h) should represent the upper limit on oven B-stage conditions.
(3) The predominant 2 and 5% weight losses, respectively, for specimens A and B are attributed to continuous solvent depletion from the matrix resin. Therefore, the thermal history of specimen C (250°C/1 h) should represent the lower limit on oven B-stage conditions.
(4) For specimen C, 2% weight loss occurred at 300°C. This temperature should represent the minimum hold temperature in the cure cycle before the consolidation pressure is safely applied. From the behaviour of specimen D, the hold time should not exceed 1.0 h at 300°C in order to take advantage of the remaining melt fluidity of the fast drying matrix resin.

Based on the above considerations, a series of four unidirectional composite panels were moulded from prepreg made with 3% offset polymer in order to determine the optimal cure cycle. Oven B-stage conditions for the prepregs used to fabricate these panels are tabulated in *Table 5*. Sixteen 7.62 cm × 7.62 cm dried prepreg plies were cut from each B-staged lot. The 16 plies were stacked and moulded in a press according to the cure cycle shown in *Figure 8*. All four panels had an identical cure cycle. Two layers of bleeder cloth were added on each side of the stacked plies in the mould. Heat-up of the press to the first hold temperature, 316°C, took about 45–60 min. A 1.72 MPa consolidation pressure was not applied until after the 30 min hold at 316°C. This was a crucial step in the design of the cure cycle, as will be seen from the results discussed below. The pressure was not relieved until the mould temperature dropped below 100°C (well below $T_g$) during the cool-down stage of the cycle.

C-scans at 5 MHz for these four panels are shown in *Figure 9*. A clear pattern of decreasing consolidation quality (increasing void content) with increasing B-stage temperature is evident. The poor C-scan of panel GD1425 (B-staged 315°C/1.0 h) is attributed to poor resin melt fluidity, not to residual solvent and/or reaction by-products. The fully imidized matrix resin (reaching a nominal $T_g$ of 255°C) was too stiff to infiltrate the fibre bundles within the laminate under a moderate consolidation pressure of 1.72 MPa. On the other hand, better C-scan patterns were achieved for panels GD1422 (B-staged 250°C/1.0 h) and GD1426 (B-staged 275°C/1.0 h) which were prepared from prepreg B-staged at less severe conditions. These panels would tend to trap more residual solvent than panel GD1425 during consolidation. This would aid in melt flow via plasticization of the matrix. However, the amount of trapped residual solvent was insufficient (≪2%) to generate voids and poor C-scan patterns. On the other hand, a hold condition much above 310°C would remove the remaining solvent and prevent good melt flow[30]. Mechanical properties of these panels will be compared in the next section.

In order to further examine the effect of oven B-stage conditions on the consolidation quality of the composite, another moulding was made where the B-stage temperature was lowered to allow more solvent to be present during the consolidation step. The oven B-stage for the prepregs was conducted at 225°C for 30 min and a slightly higher

**Table 5** Oven B-stage conditions for prepreg used in the development of an optimal cure cycle

| | 3% Offset prepreg B-stage conditions | |
|---|---|---|
| Panel | Temperature (°C) | Time (h) |
| GD1422 | 250 | 1.0 |
| GD1426 | 275 | 1.0 |
| GD1424 | 300 | 1.0 |
| GD1425 | 315 | 1.0 |

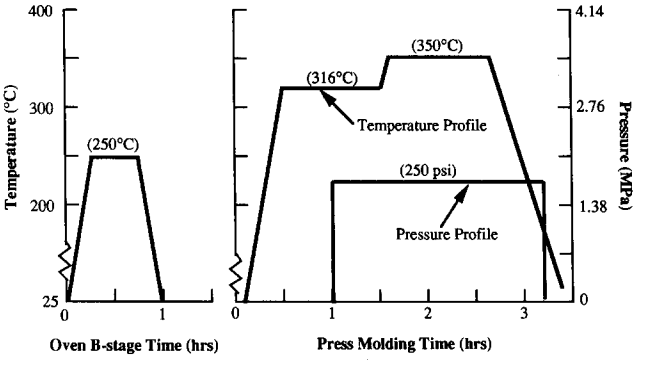


**Figure 8** Optimal moulding cycle for IM7/LARC™-ITPI composites. This cycle includes an oven B-stage step at 250°C

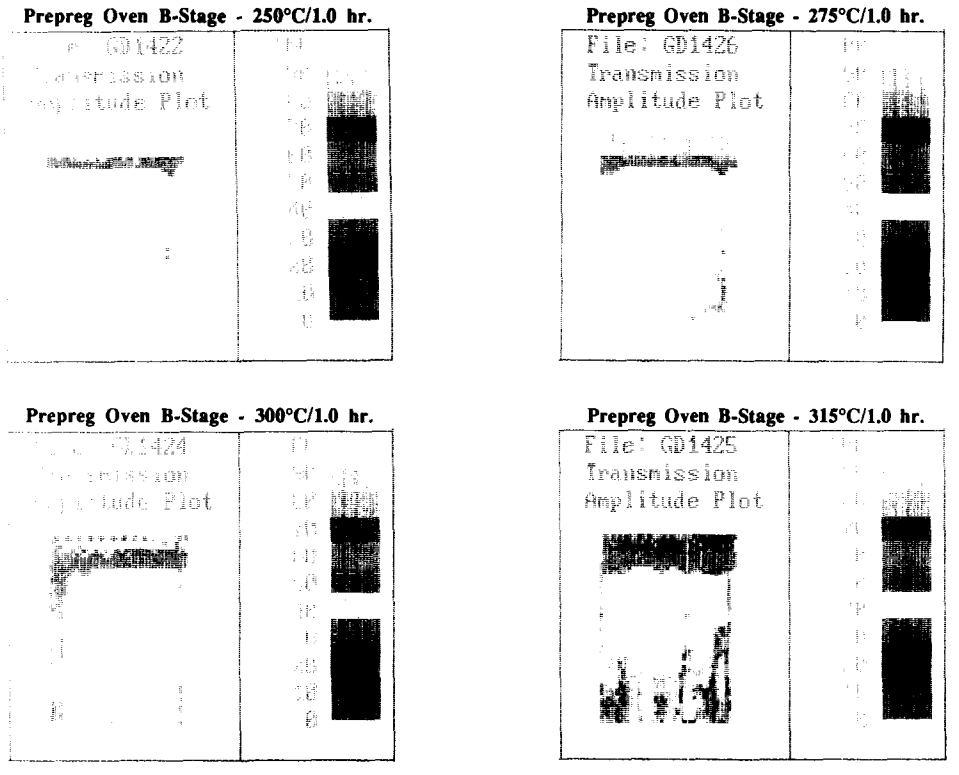


**Figure 9** C-scans for four composite panels fabricated in the parametric study to develop an optimal moulding cycle

final hold temperature (i.e.375°C vs. 350°C) was used. The cure cycle and the C-scan image of the resultant panel (GD1403) are shown in *Figure 10*. The C-scan pattern indicated poor panel consolidation. Such a result clearly demonstrated that an oven B-stage at 225°C for 30 min was inadequate for NMP removal and that a higher moulding temperature had little effect on the consolidation quality of the panel. It was conceivable that, because of the poor fluidity of the molten LARC™-ITPI, the trapped volatiles inside the laminate were difficult to squeeze out once the consolidation pressure was applied.

Short-beam shear (SBS) and 0° flexural data for the four panels described in *Table 5* are tabulated in *Table 6* along with other information about the tests. The SBS strengths measured at r.t. and 177°C did not reveal a clear relationship between oven B-stage treatments and panel consolidation. However, the SBS strengths of panel GD1425, whose prepreg was B-staged at 315°C, were clearly inferior to the others. These low values should not be attributed to the effect of residual solvent inside the panel, but rather to poor consolidation at 1.72 MPa pressure due to the inadequate fluidity of the fully imidized matrix resin. It was also noted that panels GD1422 and GD1424 possessed acceptable SBS values at r.t. and each retained over 75% of its r.t. strength at 177°C. Most of the SBS specimens in this study failed in compression, not in shear, as many thermoplastic SBS composites do. The results are employed here only to indicate trends.

A clear trend between B-stage treatment and panel consolidation was evident from the r.t. 0° flexural properties. Panel GD1422 possessed a flexural strength of 1348 MPa while a much lower strength was observed for panel GD1425 due to poor consolidation. The moduli were less discriminatory.

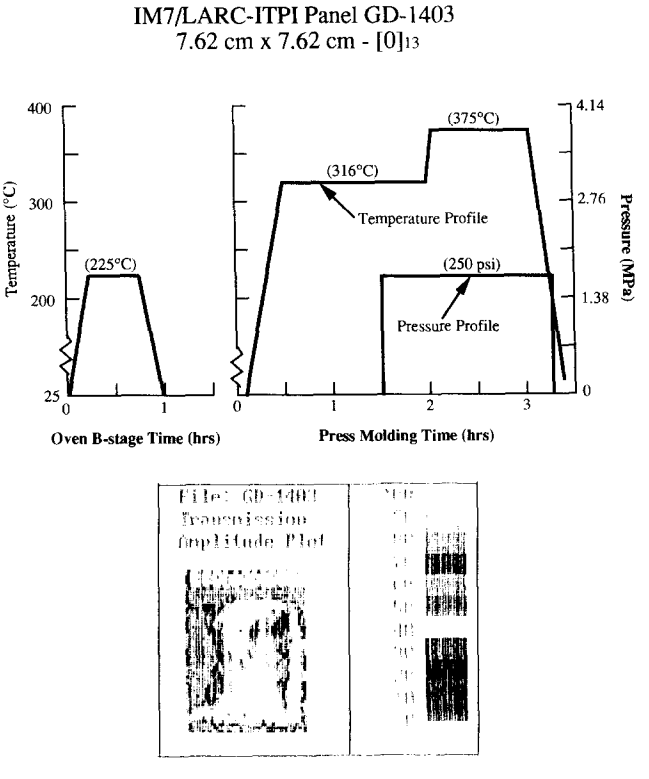


**Figure 10** Moulding cycle and C-scan image for IM7/LARC™-ITPI, composite panel GD1403

These results indicate that oven B-stage conditions for the prepreg and the initial temperature hold in the press before pressure application were the critical steps in moulding well-consolidated IM7/LARC™-ITPI composites. The moulding cycle for panel GD1422

**Table 6** Short-beam shear (SBS) and 0° flexural properties of IM7/LARC™-ITPI composites (3% stoichiometric offset) subjected to different moulding cycles

| Composite panel | | GD1422 | GD1426 | GD1424 | GD1425 |
|---|---|---|---|---|---|
| SBS at r.t. | No. of specimen | 4 | 4 | 4 | 4 |
| | Span to depth ratio | 4:1 | 4:1 | 4:1 | 4:1 |
| | Avg. SBS strength (MPa) | 88.41 | 75.89 | 97.85 | 61.05 |
| | Standard deviation (MPa) | 4.55 | 4.34 | 4.82 | 4.54 |
| | Failure mode | Mostly failed in compression | Mostly failed in compression | Mostly failed in compression | Mostly failed in compression |
| SBS at 177°C | No. of specimen | 5 | 5 | 5 | 5 |
| | Span to depth ratio | 4:1 | 4:1 | 4:1 | 4:1 |
| | Avg. SBS strength (MPa) | 67.81 | 59.26 | 76.08 | 51.13 |
| | Standard deviation (MPa) | 8.68 | 3.31 | 8.48 | 4.00 |
| | Failure mode | Mostly failed in compression | Mostly failed in compression | Mostly failed in compression | Mostly failed in compression |
| 0° Flex at r.t. | No. of specimen | 3 | 3 | 3 | 3 |
| | Span to depth ratio | 24:1 | 24:1 | 24:1 | 16:1 |
| | Avg. flexural strength (MPa) | 1348 | 1137 | 963.5 | 872.6 |
| | Standard deviation (MPa) | 6.8 | 75.3 | 53.7 | 48.1 |
| | Avg. modulus (GPa) | 76.3 | 66.1 | 64.0 | 61.5 |
| | Standard deviation (GPa) | 1.24 | 2.27 | 1.38 | 0.96 |
| | Failure mode | Failed on compression side | Failed on compression side | Failed on compression side | Failed on compression side |

(*Figure 8*) was optimal for this particular polymer composition, part size, part geometry and moulding technique and employs the maximum temperature and pressure allowed for many aerospace applications.

## SELECTION OF AN OPTIMAL LARC™-ITPI COMPOSITE COMPOSITION

### *Cross-sections of consolidated laminates*

The optimal cycle identified above for the 3% offset composition was used to fabricate prepreg and SBS and 0° flexural specimens from the remaining four polymers with 2, 4, 4.75 and 5.5% stoichiometric imbalances. Scanning electron photomicrographs from representative cross-sections of the five consolidated unidirectional composite panels are shown in *Figure 11*. In most cases, these panels consisted of 10 plies of prepreg. A magnification of 50× was taken on the cross-sections perpendicular to the fibre direction. The following observations were evident from these photomicrographs:

(i) the degree of parallelism within the plies increased with increasing stoichiometric offset;
(ii) the void content decreased with increasing stoichiometric imbalance;
(iii) the voids were mostly distributed along the interfaces between adjacent prepreg layers.

We can conclude that LARC™-ITPI matrix compositions having high stoichiometric offsets (>4%) process better and afford the most desirable microstructure. However, in order to understand why this microstructure occurs, a general discussion of pressure distribution within the laminate during consolidation is needed.

### *Consolidation mechanisms*

A schematic model for a composite cross-section parallel to a single fibre tow is shown in *Figure 12*. The thick, black solid strings represent filament bundles inside the fibre tow. The fibre tow is impregnated with matrix resin indicated by shaded areas adjacent to the filament bundles. Distribution of the resin matrix is non-uniform, and resin-rich and resin-starved domains are clearly depicted. In practice, the filament bundles in the prepreg are not strictly parallel; instead, numerous filament–filament contact points exist within the tow because the filaments possess a slight degree of waviness. The degree of waviness depends on the prepregging technique. Solution prepregging by drum winding, for example, would result in a higher degree of waviness among the filaments since the prepreg is removed from the drum while the matrix is still wet with solvent and the fibres lose their tension. On the other hand, frame wrapping or filament winding of towpreg would yield a lower degree of waviness (higher degree of filament parallelism) because high tension is maintained by the frame or mandrel during subsequent pressure-moulding operations.

Multi-ply thermoplastic composite laminates are commonly fabricated by the application of consolidation pressure at elevated temperatures. The temperature is usually >100°C above $T_g$. Pressure is applied to squeeze out excess resin and/or to fill the voids (resin-starved domains) within the laminate. Ideally, one would like to have the pressure effectively absorbed by the matrix resin. In reality, however, such a situation seldom occurs.

As depicted in *Figure 12*, the filaments are curved strings with numerous contact points among them. Consider the situation where the matrix resin is absent: the dry fibre structure (e.g. woven preforms) would deform as an elastic spring as load is applied. An increase in pressure would lead to a denser structure in which the filament–filament contact points increase dramatically. In this situation, non-linear behaviour between load and deformation of the fibre structure would prevail. Such a behaviour, in fact, has been observed experimentally by Gutowski *et al.*[31,32] and modelled analytically by Gutowski[33,34], Hou[35] and Batch[36]. The resin flow/fibre deformation models commonly use the following assumption in their derivations[33,35,36]:

$$P = P_r + \sigma \tag{3}$$

where $P$ is the applied pressure for composite consolidation,

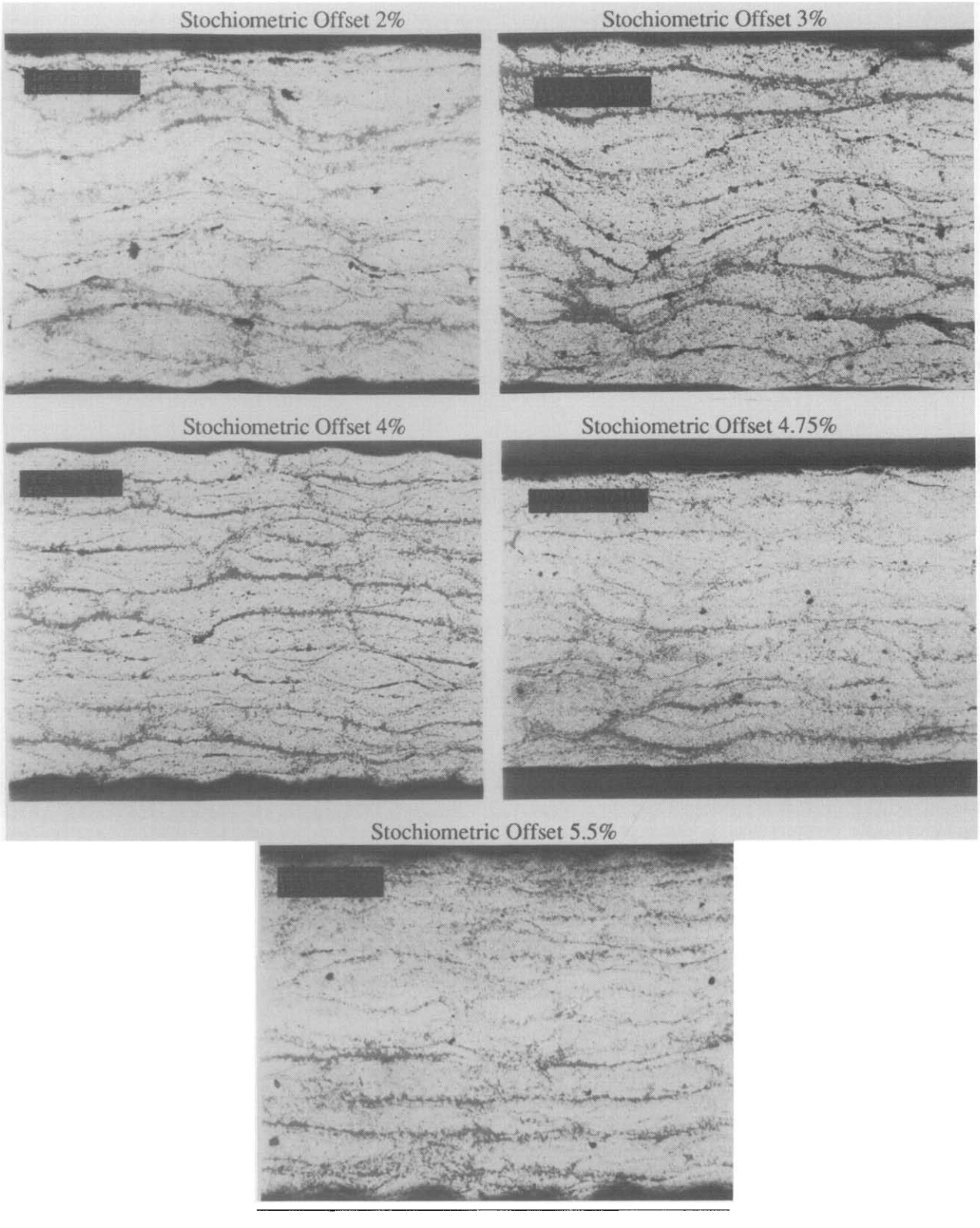


**Figure 11** Photomicrographs (50 × magnification) perpendicular to the fibre direction of consolidated IM7/LARC$^{TM}$-ITPI composites with various stoichiometric imbalances

$P_r$ is the resin pressure and $\sigma = \sigma(V_f)$ is the average effective stress in the fibres and is a function of the fibre volume fraction, $V_f$. In essence, equation (3) assumes that the fraction of the applied load absorbed by the resin and the fibre are separable and directly additive. Consequently, the elastic deformation behaviour of the fibres, $\sigma(V_f)$, can be independently measured without the presence of matrix resin. Values of $\sigma$ can then be substituted into equation (3) to calculate the required value of $P_r$ for the matrix resin to infiltrate fibre tows during consolidation.

If the model for filament–resin microstructure given in *Figure 12* is reasonably accurate, it is obvious that the assumptions in equation (3) are not accurate. Matrix resins used in high-performance composites are typically viscoelastic. The behaviour of the fibre phase is expected to be dramatically different depending on the presence of a matrix resin. In the case of a reactive matrix resin

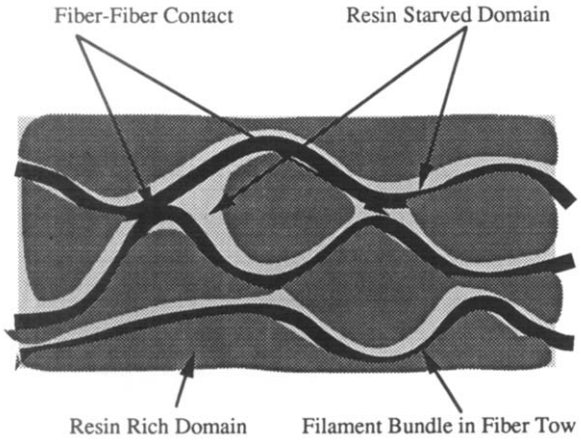


**Figure 12** Schematic diagram of fibre–resin matrix microstructure in a typical composite laminate

system, such a difference becomes time dependent. In addition, the existence of a temperature gradient (due to non-uniformity of heat transfer and/or reaction exotherm) within a composite part can lead to a non-uniform cure distribution which further complicates the viscoelastic behaviour. The uniformity of resin impregnation would also have a direct effect on the deformation behaviour during consolidation. For these reasons, the pressure distribution inside a consolidating laminate is very complex. It is extremely difficult to quantify the effects of these two interactive components (fibre and matrix resin) separately by experimental measurements.

*Consolidation of IM7/LARC™-ITPI prepreg*

During the moulding of IM7/LARC™-ITPI composites, it was shown that a 30 min hold at 315°C in the press (*Figure 8*) without pressure was a necessary and critical step for the depletion of residual NMP to a level below 2%. Consolidation pressure could then be safely applied so that formation of voids due to the excess volatiles trapped within the laminate could be avoided. Such a moulding procedure would, however, inevitably compromise the fluidity of the curing matrix resin such as LARC™-ITPI. A resin with lower stoichiometric imbalance would react to form a polymer with higher molecular weight and melt viscosity, and consequently the resin infiltration within the laminate during consolidation would become more difficult, especially under restricted consolidation pressures $< 1.72$ MPa.

It is believed that the consolidation behaviour observed in *Figure 11* for composites with the five offset stoichiometries is a direct consequence of the complex pressure distribution inside the laminate, as discussed above. To illustrate this point, a photomicrograph with enhanced magnification (200×) is shown in *Figure 13*. This photo represents a cross-section perpendicular to the fibre tows for a consolidated IM7/LARC™-ITPI panel with 2% stoichiometric imbalance. The C-scan for this panel was poor, as expected after viewing the voids shown in the related photomicrograph, *Figure 11*. Four resin-impregnated fibre tows are visible in *Figure 13*. A uniform resin distribution within the fibre tows, with only few discrete resin-starved spots, is evident. However, large voids are observed at the interface regions between adjacent fibre tows, and resin-rich areas exist near the peripheral region of each fibre tow. These voids obviously are not due to the resin starvation within the prepreg plies. We suggest that, for a viscous 2% offset LARC™-ITPI matrix resin, the pressure employed was insufficient to overcome the combined viscoelastic forces in the fibre–resin matrix and melt flow was suppressed. The gaps between adjacent fibre tows could not be closed during consolidation and the prepreg layers remained curved.

It is obvious that when consolidation pressures were constrained to 1.72 MPa or less the quality of IM7/LARC™-ITPI composites varied widely. Composites with a matrix stoichiometric imbalance lower than 4% have melt fluidities insufficient to allow vertical and lateral movement of the matrix during consolidation. Consequently, unacceptable composite microstructure is obtained.

*Preliminary composite properties*

SBS strengths and flexure properties for composites made with the five polymer compositions are given in *Figures 14*, *15* and *16*. SBS strengths are plotted in *Figure 14*. SBS strengths at r.t. peaked at 94.5 MPa and 91.7 MPa respectively, in composites made with 4 and 4.75% offsets. The standard deviations for these composites were among the smallest. Because of higher melt viscosities associated with higher matrix molecular

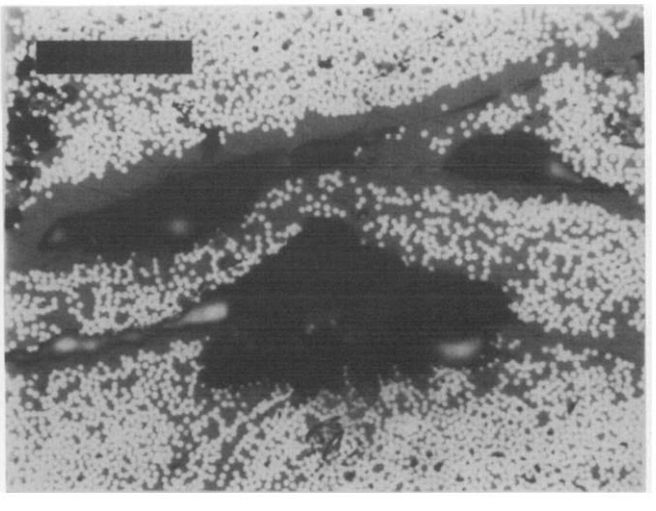

**Figure 13** Optical micrograph (200× magnification) of a representative cross-section of an IM7/LARC™-ITPI composite with 2% stoichiometric imbalance and fabricated at 1.72 MPa

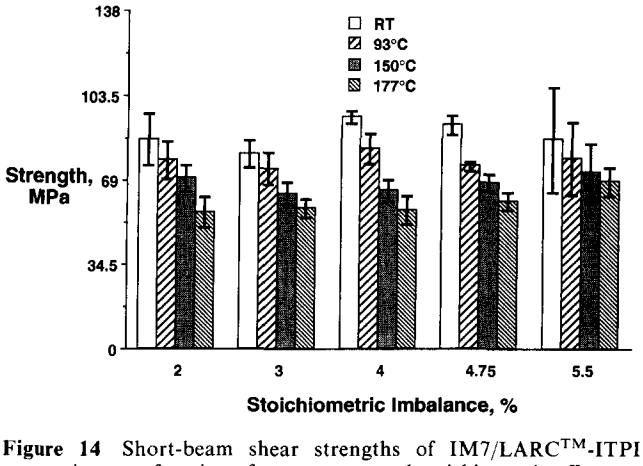


**Figure 14** Short-beam shear strengths of IM7/LARC™-ITPI composites as a function of temperature and stoichiometric offset

weights in the composites with 2 and 3% offsets, laminate consolidation was poorer, leading to lower SBS values. The non-uniformity of consolidation quality across the panels was also reflected in higher data scatter. The reason for the large scatter in the SBS values for composites with 5.5% offset is unclear.

While SBS strengths decreased at higher temperatures, as expected, retention of r.t. values at 177°C ranged from 60 to 80%, which is very impressive and clearly demonstrates the temperature capability of LARC™-ITPI composites.

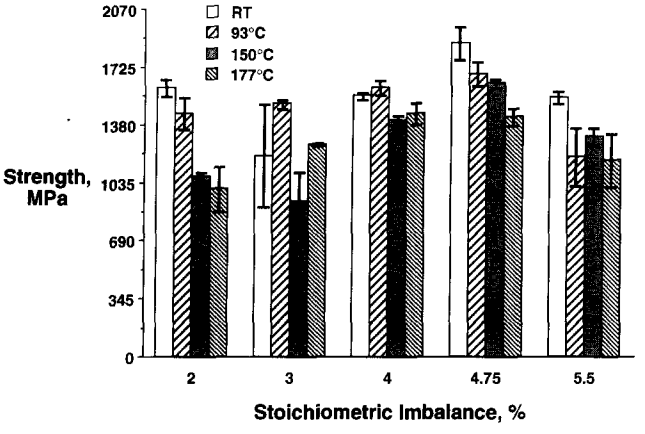


**Figure 15** 0° Flexural strengths of IM7/LARC™-ITPI composites as a function of temperature and stoichiometric offset

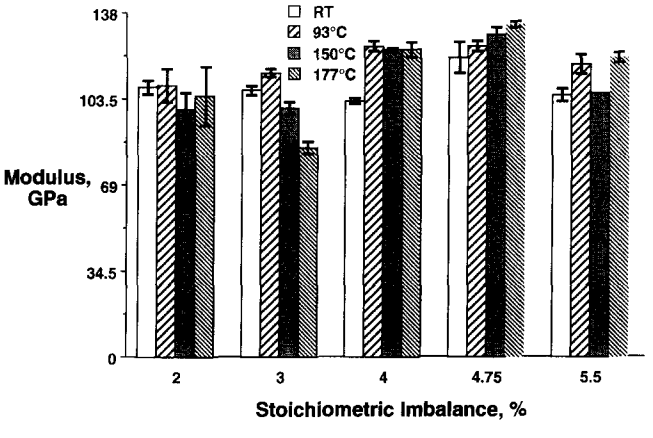


**Figure 16** 0° Flexural moduli of IM7/LARC™-ITPI composites as a function of temperature and stoichiometric offset

Longitudinal flexural strengths and moduli at both r.t. and elevated temperature maximized in composites having the 4.75% offset; the values were very respectable for IM7 fibre-reinforced laminates. The lower strength values for composites with 2, 3 and 4% offsets reflected poorer panel quality. A 76% retention of r.t. strength at 177°C was observed for the composite with 4.75% offset, again demonstrating the high-temperature capability of the LARC™-ITPI matrix.

Interlaminar fracture toughness is tabulated in *Table 7*. No readily apparent relationship was observed between polymer stoichiometric offset and composite $G_{IC}$, especially when data scatter is considered. Notably, the $G_{IC}$ for any given specimen decreased as crack length increased. This is contrary to the general trend where, as crack length increases, fibre bridging is observed and $G_{IC}$ increases. Although some bridging was evident in the post-mortem examination of these specimens, it was insufficient to dominate the test results. The $G_{IC}$ values for these composites were typically high (1.2–1.9 kJ m$^{-2}$), as would be expected for thermoplastic matrices.

These results demonstrate unequivocally that, from among the five polymer variations studied, composites fabricated from polymer with 4.75% offset stoichiometry were better consolidated and afforded the best mechanical properties, both at r.t. and at elevated temperature.

## COMPOSITE ENGINEERING PROPERTIES

More extensive engineering and design properties were determined for the composites fabricated with the 4.75% offset stoichiometry. Laminate stacking sequence, specimen size and quantity, and resin content for the composites used in these tests are summarized in *Table 8*. Similar data on the SBS, flexural and DCB tests discussed in the previous section are also included.

The engineering properties are summarized in *Table 9*. The 0° tensile properties are very good for IM7

**Table 7** Double cantilever beam (DCB) interlaminar fracture toughness, $G_{IC}$, for IM7/LARC™-ITPI composites at r.t.

| Stoichiometric offset (%) | Specimen | DCB fracture toughness, $G_{IC}$ (kJ m$^{-2}$) Crack extension number 1 | 2 | 3 | 4 | 5 | 6 | Average (kJ m$^{-2}$) | St. Dev. (kJ m$^{-2}$) | Overall average (kJ m$^{-2}$) | Overall st. dev. (kJ m$^{-2}$) |
|---|---|---|---|---|---|---|---|---|---|---|---|
| 2 | 1 | 2.431 | 2.554 | 2.195 | 1.945 | 1.770 | | 2.179 | 0.326 | | |
| | 3 | 1.760 | 1.848 | 1.624 | 1.395 | 1.460 | | 1.617 | 0.192 | 1.887 | 0.33 |
| | 5 | 2.125 | 1.902 | 1.954 | 1.695 | 1.647 | | 1.865 | 0.196 | | |
| 3 | 1 | 1.819 | 1.003 | 1.457 | | | | 1.427 | 0.409 | | |
| | 3 | 1.442 | 1.386 | 1.216 | 2.511 | | | 1.639 | 0.589 | 1.466 | 0.424 |
| | 5 | 1.349 | 1.595 | 1.581 | 1.423 | 0.810 | | 1.352 | 0.320 | | |
| 4 | 1 | 1.369 | 1.605 | 1.575 | 1.606 | 1.192 | | 1.469 | 0.184 | | |
| | 3 | 2.391 | 2.224 | 1.661 | 1.634 | 1.619 | | 1.906 | 0.372 | 1.676 | 0.293 |
| | 5 | 1.768 | 1.717 | 1.655 | 1.544 | 1.581 | 1.488 | 1.653 | 0.093 | | |
| 4.75 | 1 | 1.008 | 1.479 | 1.420 | 0.930 | 0.965 | | 1.176 | 0.257 | | |
| | 3 | 1.288 | 1.121 | 1.264 | 1.183 | 1.135 | | 1.198 | 0.075 | 1.214 | 0.157 |
| | 5 | 1.333 | 1.361 | 1.161 | 1.310 | 1.166 | | 1.267 | 0.096 | | |
| 5.5 | 1 | 0.989 | 1.524 | 1.976 | 1.226 | | | 1.429 | 0.425 | | |
| | 3 | 1.275 | 1.209 | 1.159 | 1.074 | 1.063 | | 1.156 | 0.090 | 1.277 | 0.304 |

**Table 8** Mechanical test plan for IM7/LARC™-ITPI composites[a]

| | Mechanical test | Laminate stacking sequence | Length (cm) | Width (cm) | Test temp. (°C) | No. specimen at each temp. | Resin content (% w/w) |
|---|---|---|---|---|---|---|---|
| 1 | SBS | $[0]_{20}$ | 1.91 | 0.64 | r.t., 93, 150, 177 | 7 | 37.8 |
| 2 | 0° Flexural | $[0]_{10}$ | 6.99 | 1.27 | r.t., 93, 150, 177 | 5 | 38.2 |
| 3 | DCB (25.4 mm × 12.7 μm flaw in mid-plane) | $[0]_{24}$ | 15.24 | 2.54 | r.t. | 3 | 35.8 |
| 4 | 0° Tension | $[0]_8$ | 15.24 | 1.27 | r.t. | 3/5 | 36.0 |
| 5 | 90° Flexural | $[90]_{10}$ | 2.54 | 1.27 | r.t., 93, 150, 177 | 3/4 | 44.3 |
| 6 | Interlaminar shear | $[\pm 45]_{2s}$ | 15.24 | 1.91 | r.t., 177 | 3/4 | 39.2 |
| 7 | 0° Compression (IITRI) | $[0]_{16}$ | 15.24 | 1.27 | r.t. | 5 | – |
| 8 | SBC | $[-45/0/45/90]_{4s}$ | 4.45 | 3.81 | r.t., 177 | 4 | 39.6 |
| 9 | CAI | $[-45/0/45/90]_{4s}$ | 15.24 | 10.16 | r.t. | 2 | 39.6 |
| 10 | OHC (6.35 mm dia. hole in centre) | $[-45/0/45/90]_{2s}$ | 30.48 | 3.81 | r.t., 177 | 3 | 31.4 |

[a]Specimens for tests 1–5 and 7 were moulded at 1.72 MPa; specimens for tests 6, 8 and 9 were moulded at 6.88 MPa; specimen for test 10 was moulded at 3.44 MPa

**Table 9** Summary of engineering mechanical properties of IM7/LARC™-ITPI composites

| Measurement | Condition (°C) | IM7/LARC™-ITPI (4.75% offset) |
|---|---|---|
| 0° Tension strength (MPa) | r.t. | 2371 |
| Modulus (GPa) | r.t. | 137.8 |
| 90° Flexural strength (MPa) | r.t. | 108.9 |
| | 93 | 83.4 |
| | 150 | 73.1 |
| | 177 | 75.8 |
| 90° Flexural modulus (GPa) | r.t. | 3.38 |
| | 93 | 2.83 |
| | 150 | 2.48 |
| | 177 | 2.83 |
| Interlaminar shear strength (MPa) | r.t. | 146.8 |
| | 177 | 111.6 |
| Modulus (GPa) | r.t. | 17.09 |
| | 177 | 12.06 |
| 0° Compression strength (MPa) | r.t. | 1088 |
| Modulus (GPa) | r.t. | 124.0 |
| SBC strength (MPa) | r.t. | 560.2 |
| | 177 | 331.6 |
| Modulus (GPa) | r.t. | 47.7 |
| | 177 | 44.4 |
| CAI strength (MPa) | r.t. | 292.9 |
| Modulus (GPa) | r.t. | 49.5 |
| OHC strength (MPa) | r.t. | 337.7 |
| | 177 | 261.9 |

composites and indicate a good translation of fibre properties into the composite. The 90° flexural data, often a barometer of resin/fibre adhesion, are also good as are the interlaminar shear strengths. The 0° and quasi-isotropic short-block compression values are average for thermoplastic composites but low compared to similar data for thermoset (epoxy) composites. The CAI and OHC strengths are excellent and show that the LARC™-ITPI composites have good damage tolerance. The 78% retention of r.t. OHC strength at 177°C is outstanding.

## REFERENCES


1 Product Information, Mitsui Toatsu Chemicals, Inc., New York
2 St. Clair, T. L. and Progar, D. L. *Polym. Prepr.* 1975, **16**(1), 538
3 Bell, V. L., Stump, B. L. and Gager, H. *J. Polym. Sci., Polym. Chem. Edn.* 1976, **14**, 2275
4 St. Clair, A. K. and St. Clair, T. L. *SAMPE Q.* 1981, **13**-1, 20
5 Burks, H. D. and St. Clair, T. L. *J. Appl. Polym. Sci.* 1985, **30**, 2401
6 Burks, H. D., St. Clair, T. L. and Progar, D. J. NASA TM 86416, Langley Research Center, 1985
7 Burks, H. D., St. Clair, T. L. and Progar, D. J. in 'Proceedings of the 2nd International Conference on Polyimides', SPE Proceedings of Recent Advances in Polyimide Science and Technology, 1987, p. 150
8 Maudgal, S. and St. Clair, T. L. *Int. J. Adhesion Adhesives* 1984, **4**(2), 87
9 Progar, D. J., St. Clair, T. L. and Pratt, J. R. in 'Polyimides: Materials, Chemistry and Characterization' (Eds C. Feger, M. M. Khojasteh and J. E. McGrath), Elsevier, New York, 1989, p. 151
10 St. Clair, T. L., Pratt, J. R., Stoakley, D. M. and Burks, H. D. in 'Polyimides: Materials, Chemistry and Characterization' (Eds C. Feger, M. M. Khojasteh and J. E. McGrath), Elsevier, New York, 1989, p. 243
11 Burks, H. D. and St. Clair, T. L. *SAMPE Q.* 1987, **19**-1, 1
12 Johnston, N. J., St. Clair, T. L., Baucom, R. M. and Towell, T. W. *Sci. Adv. Mater. Process Eng. Ser.* 1989, **34**, 976
13 Johnston, N. J., St. Clair, T. L., Baucom, R. M. and Towell, T. W. NASA TM-101568, Langley Research Center, 1989
14 Ohta, M., Tamai, S., Towell, T. W., Johnston, N. J. and St. Clair, T. L. *Sci. Adv. Mater. Process Eng. Ser.* 1990, **35**, 1030
15 Pratt, J. R., Blackwell, D. A., St. Clair, T. L. and Allphin, N. L. *Polym. Eng. Sci.* 1989, **29**(1), 63
16 Pratt, J. R., St. Clair, T. L. and Progar, D. J. US Patent 4,937,317, 1990
17 Pratt, J. R. and St. Clair, T. L. *SAMPE J.* 1990, **26**(6), 29
18 Hou, T. H., Johnston, N. J. and St. Clair, T. L. *Sci. Adv. Mater. Process Eng. Ser.* 1993, **38**, 334
19 Carlsson, L. A. and Pipes, R. B. 'Experimental Characterization of Advanced Composite Materials', Prentice-Hall, Englewood Cliffs, 1987, p. 163
20 Siochi, E. J. and St. Clair, T. L. unpublished data, NASA Langley Research Center, 1993
21 Dine-Hart, R. A. and Wright, W. W. *J. Appl. Polym. Sci.* 1967, **11**, 609
22 Bel'nikevich, N. G., Adrova, N. A., Korzhavin, L. N., Koton, M. M., Panov, Yu. N. and Frenkel, S. Ya. *Polym. Sci. USSR* 1973, **15**(8), 2057
23 Kilhenny, B. W. and Cercena, J. L. 'Polyimides: Materials, Chemistry and Characterization' (Eds C. Ferger, M. M. Khojastech and J. E. McGrath), Elsevier, Amsterdam, 1989, p. 321
24 Volksen, W. and Cotts, P. M. 'Polyimides: Synthesis, Characterization, and Applications' Vol 1 (Ed. K. L. Mittal), Plenum Press, New York, 1982, p. 163
25 Billmeyer, F. W. 'Textbook of Polymer Science' 3rd edn, Wiley, New York, 1984
26 Hou, T. H., Johnston, N. J. and St. Clair, T. L. *Sci. Adv. Mater. Process Eng. Ser.* 1994, **39**, 573
27 Hou, T. H. and Bai, J. M. *High Perf. Polym.* 1989, **1**(3), 191
28 Hou, T. H., Wilkinson, S. P., Johnston, N. J., Pater, R. H. and Schneider, T. L. *Sci. Adv. Mater. Process Eng. Ser.* 1994, **39**, 560

29 Hou, T. H., Jensen, B. J. and Bai, J. M. *High Perf. Polym.* 1989, **1**(1), 41
30 Hou, T. H. and Johnston, N. J. unpublished data, NASA Langley Research Center, 1993
31 Gutowski, T. G., Kingery, J. and Boucher, D. 'Proceedings of the Society of Plastic Engineers ANTEC '86', 1986, p. 1316
32 Gutowski, T. G., Cai, Z., Kingery, J. and Wineman, S. J. *SAMPE Q.* 1986, **17**(4), 54
33 Gutowski, T. G. *SAMPE Q.* 1985, **16**(4), 58
34 Gutowski, T. G., Morigaki, T. amd Cai, Z. *J. Compos. Mater.* 1987, **21**, 172
35 Hou, T. H. 'Proceedings of the Society of Plastic Engineers ANTEC '86', 1986, p. 1300
36 Batch, G. L. PhD Dissertation, University of Minnesota, 1989